(This is a sample cover image for this issue. The actual cover is not yet available at this time.)

Deep-Sea Research I 58 (2011) 757–767

Contents lists available at ScienceDirect

Deep-Sea Research I

journal homepage: www.elsevier.com/locate/dsri

Instruments and Methods

Volumetric mapping of tubeworm colonies in Kagoshima Bay through autonomous robotic surveys

Toshihiro Maki *, Ayaka Kume, Tamaki Ura

Institute of Industrial Science, The University of Tokyo, 4-6-1 Komaba, Meguro-ku, Tokyo 153-8505, Japan

ARTICLE INFO

Article history:
Received 12 February 2011
Received in revised form
15 May 2011
Accepted 18 May 2011
Available online 26 May 2011

Keywords:
Tubeworm
3D mapping
Image processing
Biomass estimation
Autonomous underwater vehicles

ABSTRACT

We developed and tested a comprehensive method for measuring the three-dimensional distribution of tubeworm colonies using an autonomous underwater vehicle (AUV). We derived volumetric measurements such as the volume, area, average height, and number of tubes for colonies of *Lamellibrachia satsuma*, the world's shallowest-dwelling vestimentiferan tubeworm discovered at a depth of 82 m, at the Haorimushi site in Kagoshima Bay, Japan, by processing geometric and visual data obtained through low-altitude surveys using the AUV *Tri-Dog* 1. According to the results, the tubeworm colonies cover an area of 151.9 m^2, accounting for 5.8% of the observed area (2600 m^2). The total number of tubes was estimated to be 99,500. Morphological parameters such as area, volume, and average height were estimated for each colony. On the basis of average height, colonies could be clearly separated into two groups, short (0.1–0.3 m) and tall (0.6–0.7 m), independent of the area.

1. Introduction

Quantitative mapping of benthic habitats is the fundamental measure for scientific fisheries management (Pikitch et al., 2004), monitoring environmental change, and assessing the impact of human disturbance on benthic organisms (Ingole et al., 2001; Myers and Ambrose, 2009). Furthermore, it is the key step to evaluate the contribution of benthic organisms to the global carbon cycle (Falkowski, 2000; Lebrato et al., 2010). Collection of fine bathymetric and imagery data of the seafloor is a fundamental requirement for quantitative measurements. However, this is currently a costly process that requires the use of ROVs, HOVs, or towing sleds, which can cover only a limited area (Courtney et al., 2007; Sanchez et al., 2009). Furthermore, it is especially difficult to acquire geometrically accurate image mosaics over areas much larger than the field of view. As a result, spatial distribution of benthic habitats has to be estimated from a sparse set of images (Ierodiaconou et al., 2007; Kostylev et al., 2001).

An AUV is a self-contained, tether-free, and automated platform (Nicholson and Healey, 2008). AUVs are suitable for seafloor mapping as they can perform stable surveys with homogeneous image quality for as long as their power sources last. As underwater robotic technologies have advanced, an increasing number of AUVs have been deployed for seafloor imaging (Johnson-Roberson et al., 2010; Singh et al., 2004; Yoerger et al., 2007). Although the vast amount of information provided by these AUVs is likely to bring significant benefits to both the scientific and industrial communities, excess information also leads to the problem of information explosion. Automatic data processing and analysis are then essential technologies for coping with this problem.

This paper proposes a comprehensive method for performing a volumetric mapping of tubeworms, key benthic organisms at hydrothermal vent fields and cold seeps, over thousands of square meters using an AUV. Quantitative evaluation of tubeworm biomass is essential not only for characterizing the site in the context of biology but also for evaluating the geological activity of the site, given that tubeworms are dependent on fluid and gas seepage or hydrothermal venting (Boetius, 2005; Cardigos et al., 2005; Tarasov et al., 2005). Although the method cannot distinguish occupied from vacant tubes, it provides a fundamental dataset for biomass estimation. On the other hand, there is a fundamental need to measure growth of biogenic reefs without necessarily estimating biomass (Degraer et al., 2008).

The method measures the three-dimensional distributions of tubeworm colonies through fine-scale bathymetry and imagery with precise relative positioning in real time. Fig. 1 shows an overview of the method. First, the AUV takes pictures and collects fine bathymetric data of the seafloor through dense low-altitude scanning. Our navigation algorithm enables the AUV to follow the rugged seafloor at a close range suitable for visual surveys.

Abbreviations: ROV, remotely operated vehicle; HOV, human occupied vehicle; AUV, autonomous underwater vehicle; DVL, Doppler velocity log; FOG, fiber-optic gyro; INS, inertial navigation system; SLAM, simultaneous localization and mapping; FFT, fast Fourier transformation

* Corresponding author. Tel.: +81 3 5452 6904; fax: +81 3 5452 6489.
E-mail address: maki@iis.u-tokyo.ac.jp (T. Maki).

0967-0637/$ - see front matter © 2011 Elsevier Ltd. All rights reserved.
doi:10.1016/j.dsr.2011.05.006

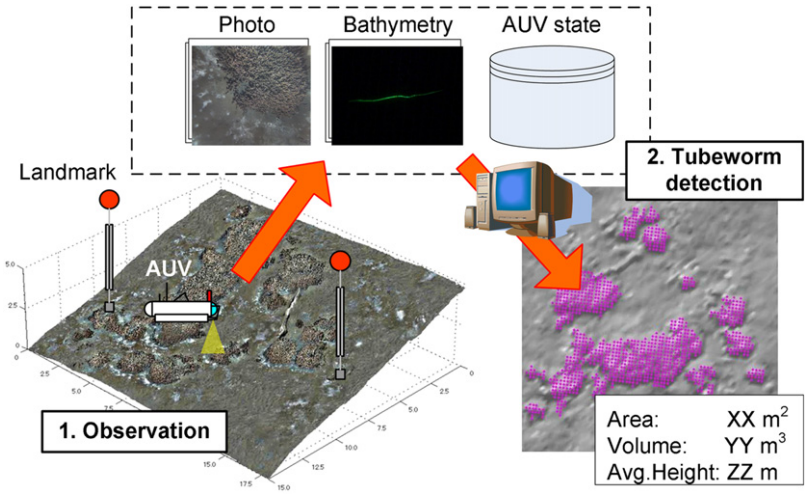

Fig. 1. Overview of the proposed method. The method is divided into the two phases of (1) observation by an AUV and (2) post-processing for tubeworm detection. Two artificial landmarks are required for navigation of the AUV.

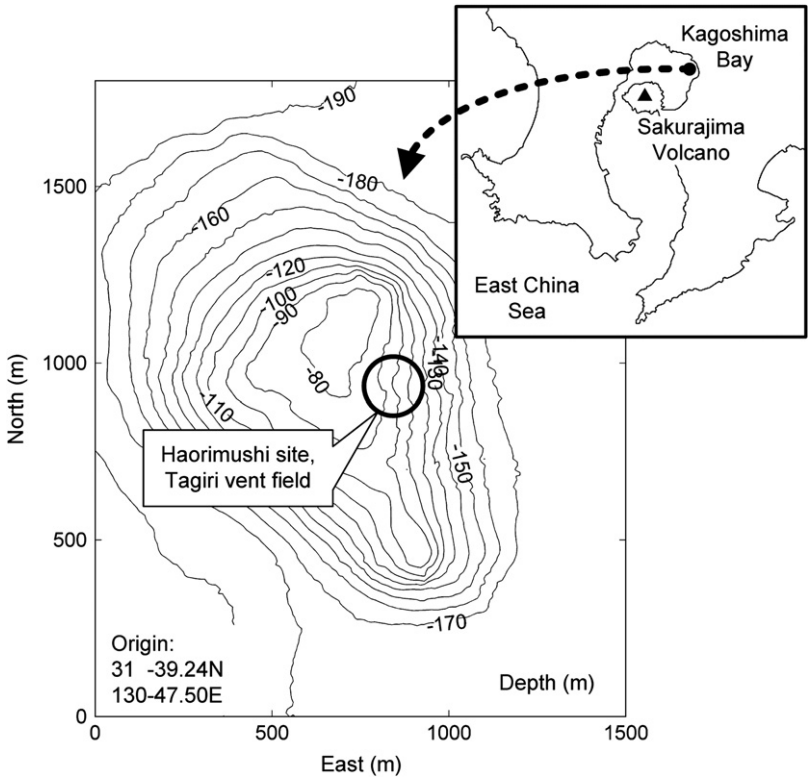

Fig. 2. Haorimushi site in Kagoshima Bay, Japan.

The horizontal position and heading of the vehicle are estimated in real-time according to artificial landmarks. The three-dimensional distribution of tubeworm colonies is then obtained through the two steps of geometry-based estimation and image-based verification. Finally, quantitative values such as the area, volume, and average height of the colonies are calculated.

The AUV *Tri-Dog* 1 has been periodically deployed to the Tagiri vent field in Kagoshima Bay, Japan. The depth of the site is around 100 m, and colonies of *Lamellibrachia satsuma* exist there. This paper reports the spatial distribution of the tubeworm colonies at the site over an area as large as 2,600 m^2 based on data obtained by a series of deployments in 2007.

1.1. *Lamellibrachia satsuma*

L. satsuma (Miura et al., 1997) is the shallowest-dwelling vestimentiferan tubeworm discovered at the depth of 82 m around a seep site named "Haorimushi site", located on the east side of a knoll neighboring on the Wakamiko Proto-caldera in the northeast part of Kagoshima Bay, Japan (Fig. 2). Vestimentiferan tubeworms are typical members of the biological communities supported by chemosynthetic production. Surveying their distribution in both the spatial and temporal domains is important for understanding not only these organisms in their own right but also the geological mechanisms that sustain their life. Given that tubeworms are

typically found at depths greater than the euphotic zone, the study of an euphotic vestimentiferan could be relevant for a better understanding of tubeworm speciation and dispersal.

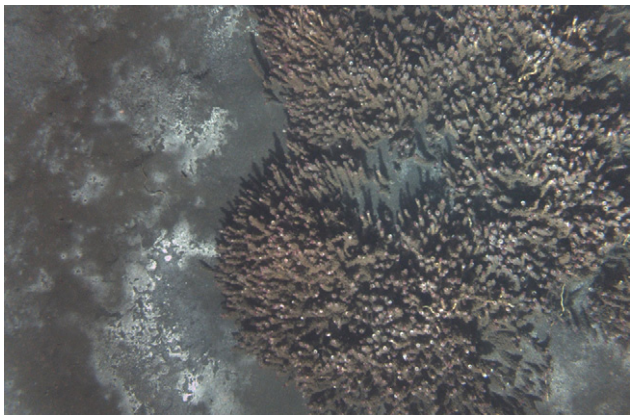

Fig. 3. Colony of *Lamellibrachia satsuma* (Miura et al., 1997) at Haorimushi site, Kagoshima Bay, photographed by the AUV *Tri-Dog* 1. The actual width of the image is approximately 2 m.

Table 1
Specifications of the autonomous underwater vehicle *Tri-Dog* 1.

Vehicle	
Size	2.0 m (L) × 0.9 m (H) × 0.6 m (W)
Mass	200 kg
Max. speed	0.7 m s^{-1}
Max. depth	110 m
Duration	4 h
Actuators	100 W thruster × 6
Communication	Wireless LAN, Acoustic modem
Sensor	
Doppler velocity log	RDI Navigator 1200 kHz
Depth	Druck PTX1830
Roll & Pitch	Crossbow AHRS 400MA
Heading	JAE JG-35FD (FOG)
Landmark search	Imagenex 881A Profiler
Payload	
Forward camera	SONY EVI-D100
Downward camera	PGR Scorpion
Bathymetry camera	SONY XC555
Sheet laser	Crown CRGS-1015L60D × 2
Lighting	Arc lamp × 2 (forward), flash × 2 (downward)

A colony of *L. satsuma* is shown in Fig. 3. The length of the individuals is about 50–100 cm, with some reaching 200 cm. It differs from other congeneric species in having a short vestimentum, a short obturaculum, up to 4 pairs of lamellar sheaths, and up to 19 pairs of branchial lamellar sheaths (Miura et al., 1997). Regarding their full bathymetric range, it is noticeable that this taxon could reach bathyal depths such as the Kanesu-no-se Bank in the Nankai Trough (depth: 270–300 m, cold seep) and the Nikko Seamount in the area north of the Mariana Islands (depth: 400–500 m, hydrothermal vent) (Fujikura et al., 2008).

A series of ROV and HOV surveys has revealed that the horizontal span of the tubeworm habitat at the Haorimushi site is 360 × 200 m, with the depth range of 76–123 m. The size of the biggest colony was reported to exceed 10 m in diameter and 5 m in height. The highest population density was estimated to be 3000 m^{-2} and the maximum biomass was suggested to surpass 15 kg m^{-2} in wet weight (Hashimoto et al., 1995; Hashimoto et al., 1993). However, detailed volumetric information such as shape of each colonies and spatial relationship among colonies remain unclear, which is useful for quantitative estimation of entire biomass, and for evaluating relationship between environmental condition and population size in local scale.

1.2. AUV Tri-Dog 1

Tri-Dog 1 is a hovering-type AUV with six thrusters that independently control surge, sway, heave, and yaw motions (Kondo et al., 2001). Its specifications are summarized in Table 1. The vehicle consists of three pressure hulls with the central one for electronics and the bottom two for batteries. Ground speed is measured by a DVL, and yaw angular velocity is measured by a FOG. Six acoustic range sensors are mounted for obstacle detection and terrain tracking. Fig. 4 depicts the location and direction of the imaging apparatus mounted on the vehicle. There are two cameras looking downward; the forward one is for seafloor imaging, and the middle one is used in combination with the sheet laser to obtain fine bathymetric data according to the light-sectioning method (Kondo et al., 2004; Tetlow and Allwood, 1995). The distance between the camera and flash for seafloor imaging is set as far as possible in order to reduce the marine snow effect, the problems of backscatter caused by suspended particles such as algae, plankton, and sand.

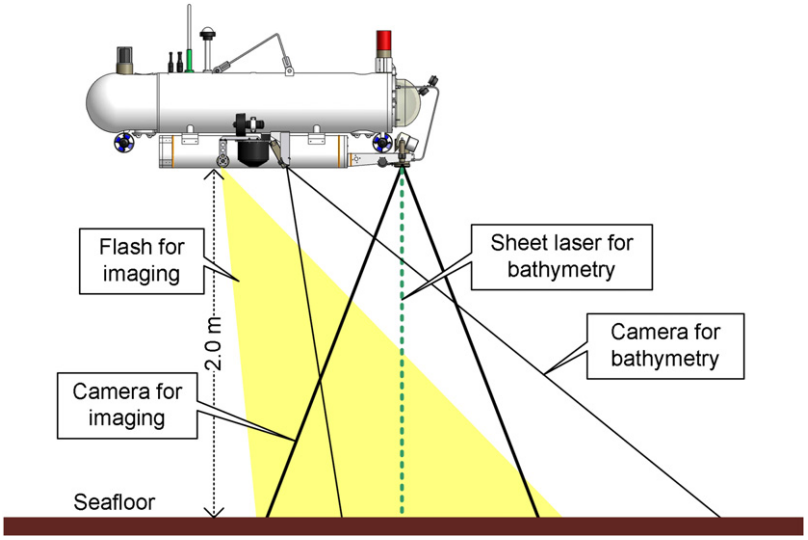

Fig. 4. Imaging apparatus mounted on the AUV *Tri-Dog* 1. Right battery hull is omitted to show sensors behind it.

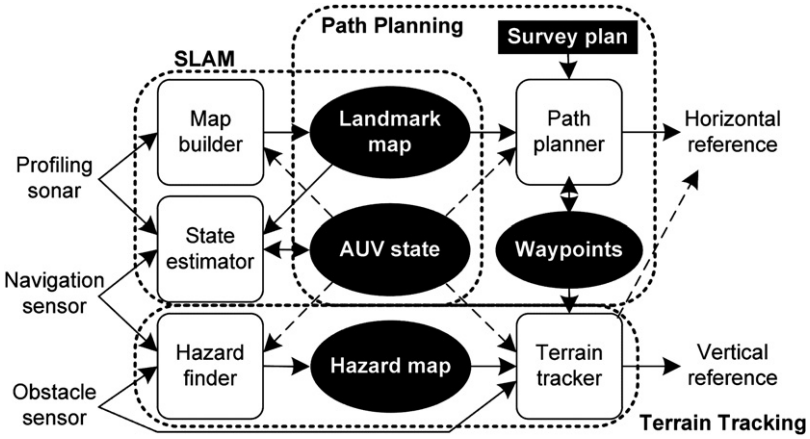

Fig. 5. Navigation scheme. The left side is input and the right side is output. Functions are surrounded by rectangles with rounded corners and the parameters are indicated by black ellipses. The arrows represent data flow.

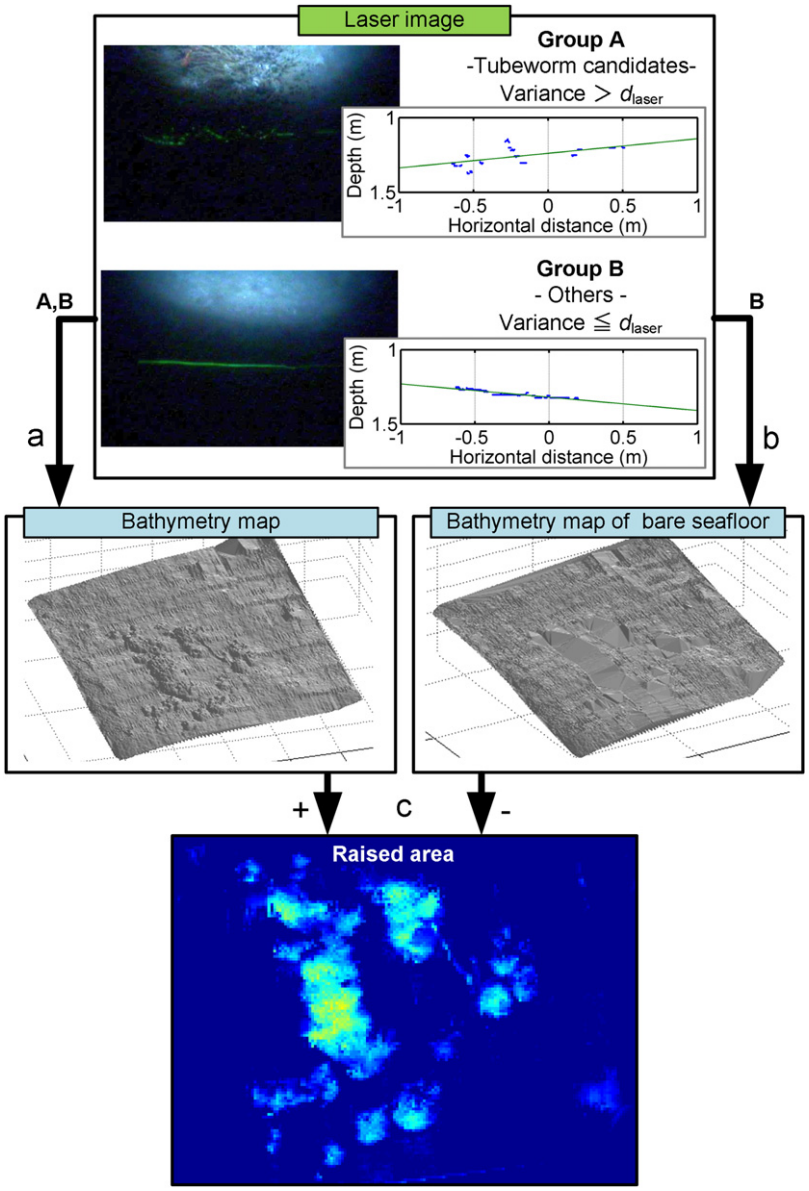

Fig. 6. Outline of geometry-based estimation. The laser image at the top contains the profile of a tubeworm colony and the next one of the bare seafloor. The blue dots in the graphs represent the profile in sensor coordinates derived from the images. The green lines are their straight-line approximation. A bathymetry map is first constructed from all of the profiles (a). Then, a bathymetry map of the bare seafloor is created using only profiles classified in group B (b). Finally, the raised area is obtained as a three-dimensional region between them (c). The raised area becomes taller as the color changes from blue to cyan, green, and yellow. (For interpretation of the references to color in this figure legend, the reader is referred to the web version of this article.)

2. Material and methods

2.1. AUV navigation

The navigation scheme enables an AUV to follow the rugged seafloor at a close range suitable for visual surveys (e.g., 2 m), with a relative positioning accuracy sufficient for photo-mosaicing. In order to achieve this, the vehicle must understand its surrounding environment, estimate its own position and attitude with regard to the environment, and take appropriate actions in real time. The key idea of the scheme is to use a profiling sonar (profiler) mounted on the AUV for positioning. *Tri-Dog* 1 is equipped with IMGENEX 881A Profiler. The profiler scans the horizontal plane with a pencil-shaped ultrasonic beam to detect landmarks. The landmarks are defined as pole-like acoustic reflectors set vertically on the seafloor as shown in Fig. 1. The horizontal position and heading of the vehicle are stochastically estimated in relation to the landmarks. A probabilistic approach is required for position estimation, because all the sensors contain stochastic errors in their measurements. Two landmarks are necessary to fix the horizontal position and heading of the vehicle. Although the working region is limited to the neighborhood of the landmarks, this method realizes accurate and drift-free positioning that is difficult for conventional methods because the range and direction of the landmarks can be directly measured. Furthermore, the method is suitable for shallow vent fields where bubble plumes exist, as they can be used as natural landmarks. The nominal maximum coverage is dependent on the detectable range of the profiler. Assuming the maximum detectable range of 100 m (it is the case for our vehicle) and the flat seafloor, the maximum coverage is approximately $300 \times 200\ m^2$, or $60{,}000\ m^2$.

The advantages of the method are as follows:

- *Self-contained*: No external aid is required once two artificial landmarks are deployed.
- *Bounded error*: The error in the horizontal position and heading are bounded as long as the vehicle stays around the landmarks, whereas the error in pure INS-based positioning increases with time.
- *Inexpensive*: Expensive INS, acoustic transponders, and hydrophone arrays are not required.
- *Robust against bubble plumes*: The method does not rely on conventional acoustic positioning schemes based on transponders and hydrophone arrays, which are weak against acoustic reflectors in the environment.

The proposed scheme consists of multiple components (Fig. 5). Detailed explanations of the three main components of the

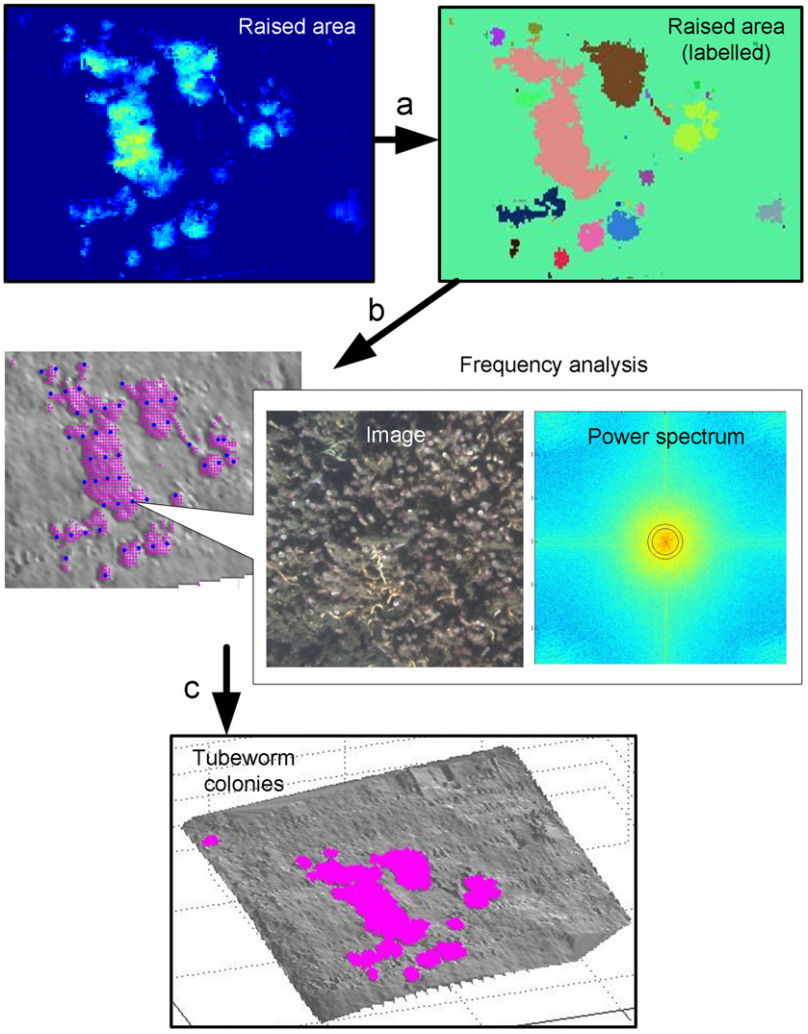

Fig. 7. Outline of image-based verification. The raised area is split into separate regions (a), where each region is in different color. Then the corresponding images are assessed according to each region (b). The blue dots on the separate regions represent center of the corresponding images. The balloon shows one of the corresponding images and its 2D power spectrum. The area between the two black circles on the spectrum is used for classification. Finally the 3D distribution of the tubeworm colonies is obtained (c). (For interpretation of the references to color in this figure legend, the reader is referred to the web version of this article.)

scheme—SLAM, path planning, and terrain tracking—can be found in previous reports (Maki et al., 2007a, 2007b, 2007c).

2.2. Tubeworm detection

The proposed method reveals the three-dimensional distribution of tubeworm colonies from a dataset consisting of the following information:

1) Seafloor images with a resolution higher than the diameter of tubeworms.
2) Bathymetric data with a resolution for each swath that is high enough to detect tubeworms.
3) Three-dimensional position and orientation of the sensors at each moment of measurement.

We cannot tell the difference between tubeworm colonies and other convex objects solely by geometric information; on the other hand, tubeworms and bacteria mats sometimes look alike judging from the spatial frequency of the images. Therefore, the method utilizes both geometry and imagery features. Although we assume bathymetry by light-sectioning, where seafloor images illuminated by a sheet-laser are the primary data, bathymetry by other instruments (profiler, multi-beam sonar, etc.) suffices as long as the resolution is sufficient. Initially, geometry-based estimation is carried out in which the tubeworm candidates are obtained from the bathymetric data as a three-dimensional region, or "raised area." Given that tubeworms form compact and knoll-like colonies, raised areas are strong candidates for tubeworm colonies. Subsequently, the raised area is split up into separate regions, each of which is then verified through frequency analysis of the corresponding seafloor images. Finally, the three-dimensional region of the tubeworm colonies is obtained, and quantitative parameters such as the area, volume, and average height are calculated.

2.2.1. Geometry-based estimation

As shown in Fig. 6, the raised areas are detected by comparing the measured bathymetry and estimated bare seafloor without protrusions. If we attempt to estimate the bare seafloor by smoothing the obtained bathymetry map, it is difficult to eliminate all protrusion effects. Furthermore, mapping artifacts are also smoothed out, which causes their inclusion in raised areas. In order to avoid these problems, individual measurements are classified before mapping. All measurements are classified into two groups—tubeworm candidates (Group A) and all others (Group B)—based on the linearity of the seafloor profile contained in each measurement. A measurement is classified in group A if

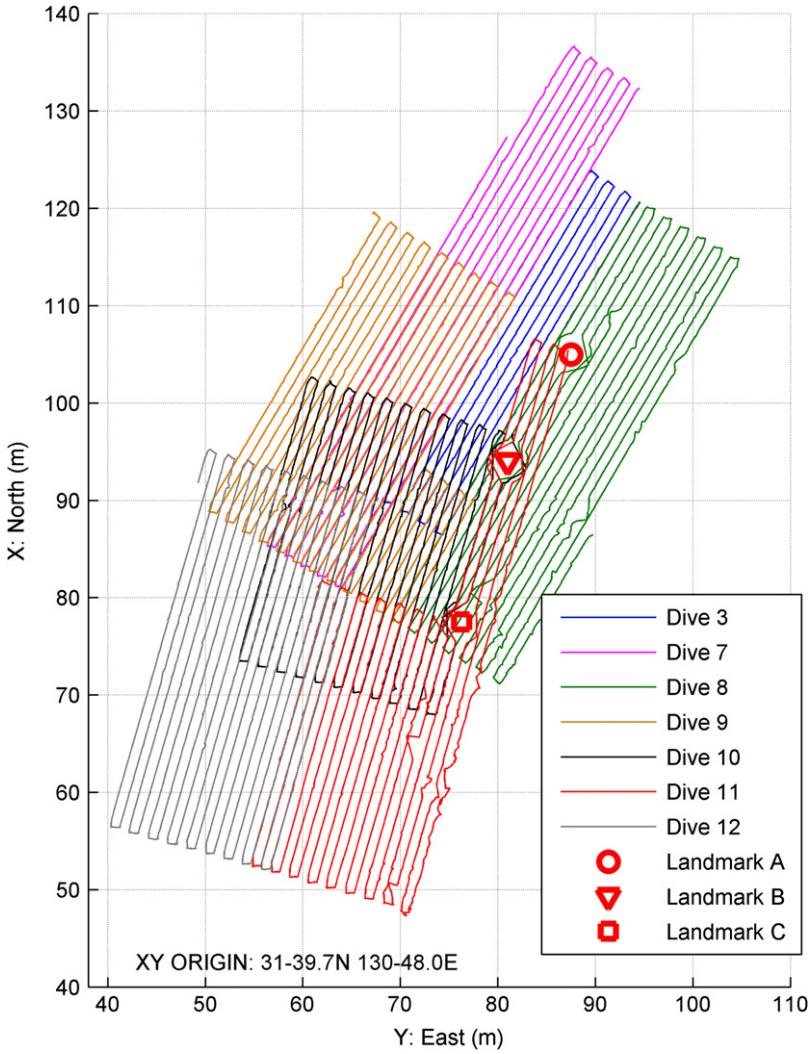

Fig. 8. Trajectory of *Tri-Dog* 1 and landmark locations estimated in real time. Landmarks A and B were used for dives 1–9, whereas landmarks B and C were used for dives 10–12. (For interpretation of the references to color in this figure legend, the reader is referred to the web version of this article.)

its variance from its linear approximation is larger than a threshold d_{laser}, otherwise, it is classified in group B.

As tubeworm colonies are compact and dense, their profile is assumed to be jagged.

A bathymetry map is first constructed from all of the measurements by transforming them to the world coordinates based on the sensor pose. Then, a bathymetry map of the bare seafloor is created using only profiles classified in group B. Blank areas in the both maps are linearly interpolated. Finally, the raised area is obtained as a three-dimensional region between the estimated bare seafloor and the original bathymetry. In order to eliminate noise, parts of the raised area with a vertical span of less than the threshold d_{raise} are cut.

2.2.2. Image-based verification

The raised area contains not only tubeworm colonies but also other objects such as bubble plumes, rocks, and refuses. Artifacts caused by sensor noise, misalignment, and positioning error are also included. The purpose of this stage is to filter out these objects based on seafloor images. The key is the spacial frequency of brightness change. Given that tubeworms have uniform diameter (6–12 mm for *L. satsuma*), brightness of tubeworm colonies are assumed to change with the frequency around their diameter, or 2D Fourier power spectra of their images become high at the corresponding frequency band.

As shown in Fig. 7, the raised area is firstly split into separate regions. Then, the corresponding images are assessed according to each region. If an image is geometrically located in one of the separate regions based on the sensor pose, it is regarded as the corresponding image of that region. The power spectrum is obtained by the two-dimensional FFT. Only the central part of each image is used, so as to reduce the spatial disparity between the raised area and the image. An image is classified as tubeworms if the sum of its power spectra inside the corresponding frequency band exceeds a certain threshold. A separate region is classified as a tubeworm colony if at least one corresponding image is judged as such.

3. Results and discussion

The proposed method was implemented using the AUV *Tri-Dog* 1 in a series of dives performed at the Haorimushi site of the Tagiri vent field in Kagoshima Bay, Japan, in 2007.

3.1. AUV deployments

The series of deployments were carried out using the R/V *Tansei-Maru* for the cruise KT07-20 during 16–26 August 2007. The vehicle succeeded in 12 dives spanning a total duration of

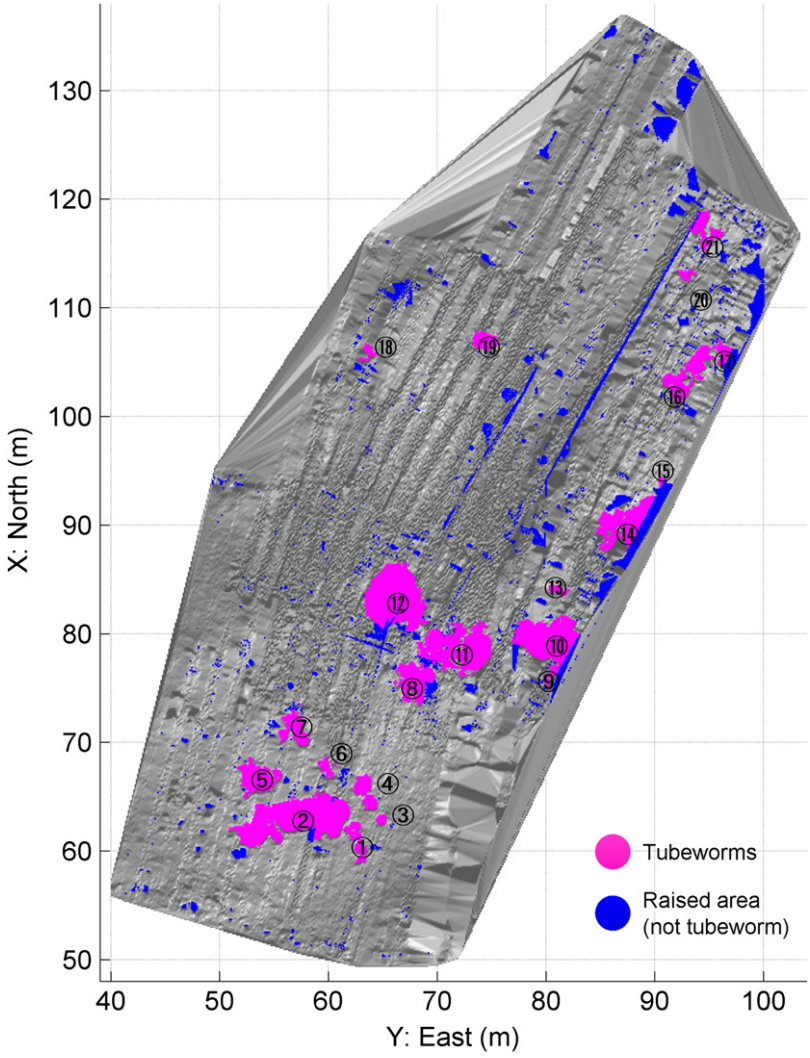

Fig. 9. Distribution of tubeworm colonies at the Haorimushi site obtained through the deployments. Colonies with areas larger than 0.1 m^2 are numbered.

29 h and obtained more than 9000 images of the seafloor. Fig. 8 shows the trajectory of the vehicle and the landmark locations estimated in real time. Landmarks A and B were used for dives 1–9, whereas B and C were used for dives 10–12. During the seafloor observations, the vehicle took a seafloor image with a flash every 8 s while taking a laser image every 1 s and maintained a surge speed of 0.08 m s^{-1}. The altitude of the vehicle was maintained at 1.2 m above the seafloor. The seven dives indicated

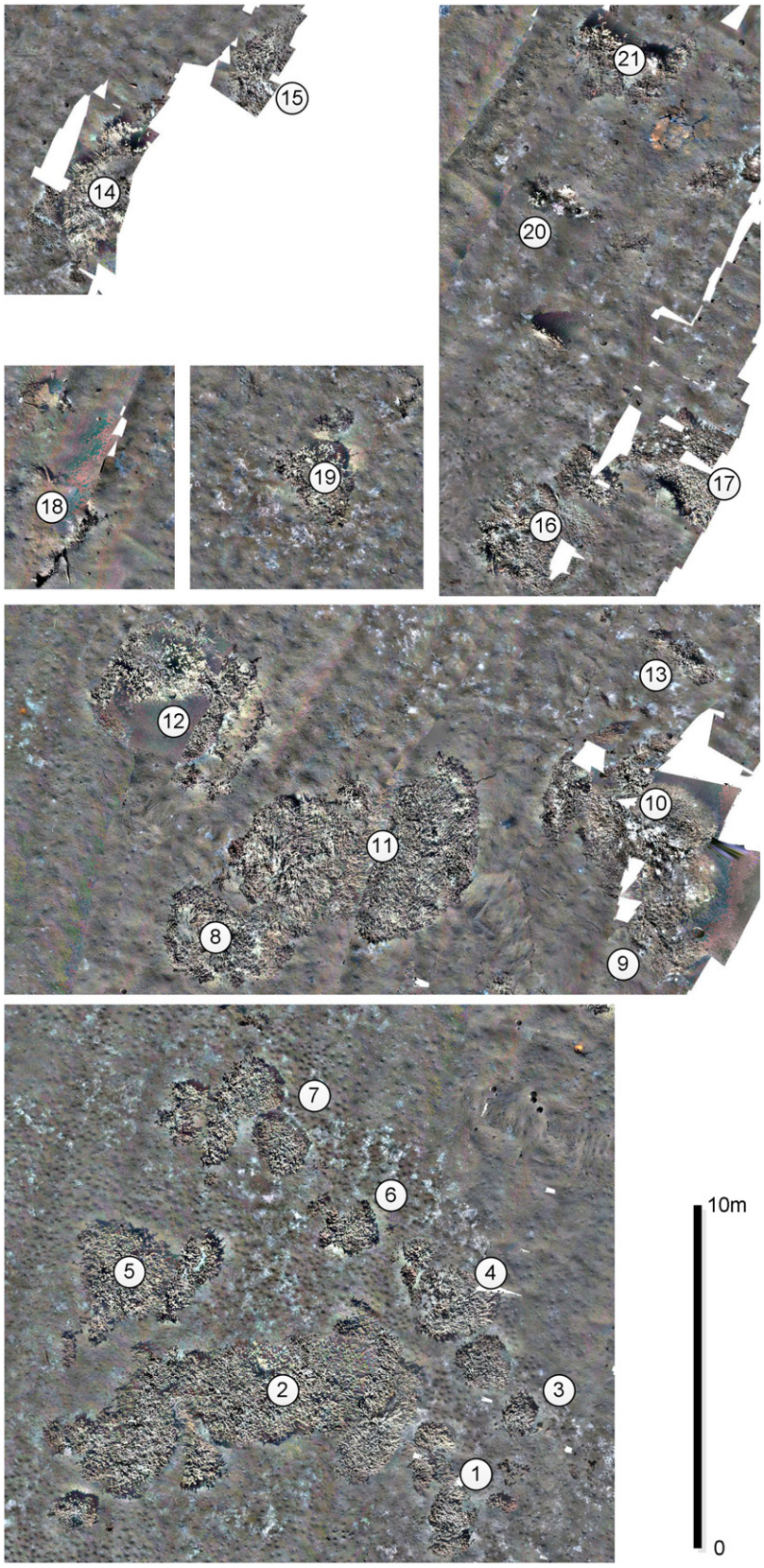

Fig. 10. Photomosaic of the seafloor of the Haorimushi site created through the deployments. The numbers indicate the corresponding tubeworm colonies shown in Fig. 9.

in Fig. 8 were used for tubeworm detection. The vehicle covered a seafloor area of 2,600 m^2 by taking 7,289 pictures during the seven dives.

3.2. Tubeworm detection

Fig. 9 shows the detected tubeworm regions mapped in the same coordinate system used in Fig. 8; the threshold d_{raise} was set as 0.09 m. The tubeworm regions are represented in magenta, whereas the raised areas defined as not tubeworms are represented in blue. Tubeworm colonies with areas of more than 0.1 m^2 are numbered. The background is the shaded bathymetry obtained from the light-sectioning measurements. According to the results, the tubeworm colonies cover an area of 151.9 m^2, which is 5.8% of the observed area.

Fig. 10 shows the photomosaics of the corresponding tubeworm colonies shown in Fig. 9. The photomosaic was created using the pictures taken by the vehicle during the seven dives; the image alignment is based simply on navigation data obtained by the vehicle, or no inter-image matching is performed. Tubeworm colonies, bacteria mats, and other features of the environment are visually recognized. A comparison of Figs. 9 and 10 indicates that all of the numbered tubeworm colonies except colony 18 were correctly detected. Although Fig. 10 reveals that colony 18 is actually a rock mound with minor patches of tubeworms, the method regarded the entire rock mound as tubeworms. This is because the classification was performed on an entire raised area. Although this is a drawback of the method, exaggerated detection is still more favorable than missing features as there is an opportunity for manual correction.

In order to evaluate the reliability of the detected colonies, the location and shape of the same colony were compared between dives. Fig. 11 shows the geometry of colony 12 obtained by dives 9 and 10. There is a horizontal offset of 1.1 m in the center of the volume. The area, volume, and average height of the colony were measured as 16.6 m^2, 11.6 m^3, 0.7 m (dive 9) and 15.0 m^2, 12.4 m^3, 0.8 m (dive 10), respectively. Based on the results, the method is assumed to have error margin of 11% in area and 13% in height. The error margin in volume is assumed to be 25%, because the volume is a product of area and height. One of the main reasons for the error is the lack of bathymetric measurements caused by the vehicle's obstacle avoidance maneuvers. Such maneuvers degrade the geometric resolution of the final results and lead to a loss of robustness against outlier measurements. The use of strong lasers for bathymetry can mitigate this problem. Another reason is the positioning error of the vehicle. The positioning reliability is affected by relationship between the vehicle and the landmarks. Environmental conditions such as the roughness and gradient of seafloor, and amount of bubble plumes also affect the reliability, since they cause noises to the sensors used for positioning. The positioning errors at the experiments were estimated to be 0.36–0.81 m by comparison of seafloor images among dives (Maki et al., 2008). The error margin of the covered area is then estimated to be 73 m^2 by multiplying the positioning error of 0.81 m by the length of the coverage, which accounts for 2.8% of the calculated covered area of 2,600 m^2.

3.3. Colony morphology

Table 2 indicates the morphological parameters for all of the numbered colonies shown in Fig. 9. The number of tubes was estimated by simply multiplying the footprint by the habitat density, which in turn was estimated manually as 655 m^{-2} based on the images taken by the vehicle. Fig. 12 represents the histograms of the parameters. According to the figure, the area and volume were widely spread between 0–30 m^2 and 0–15 m^3, respectively. The frequency decreased as the area or volume increased. On the other hand, the average height was clearly

Table 2
Quantitative values of the detected tubeworm colonies. Only those with areas larger than 0.1 m^2 are shown. The totals were calculated from all of the detected colonies. The number of tubes was estimated by multiplying the area by the visually estimated density (655 m^{-2}).

No.	Area (m^2)	Volume (m^3)	Avg. height (m)	No. of tubes
1	3.15	0.59	0.19	2066
2	29.06	8.87	0.31	19,034
3	0.68	0.14	0.21	443
4	3.61	0.77	0.21	2367
5	7.36	1.99	0.27	4820
6	1.32	0.21	0.16	868
7	4.65	1.04	0.22	3047
8	8.09	1.61	0.20	5301
9	0.26	0.04	0.15	170
10	17.84	12.48	0.70	11,686
11	18.89	3.68	0.19	12,375
12	25.06	15.05	0.60	16,412
13	1.04	0.17	0.17	679
14	11.39	6.82	0.60	7461
15	0.30	0.09	0.30	198
16	7.99	2.46	0.31	5235
17	1.83	0.41	0.22	1198
18	0.96	0.24	0.24	632
19	3.17	0.86	0.27	2075
20	0.94	0.29	0.30	613
21	3.99	1.20	0.30	2613
Total	151.93	59.03	0.39	99,517

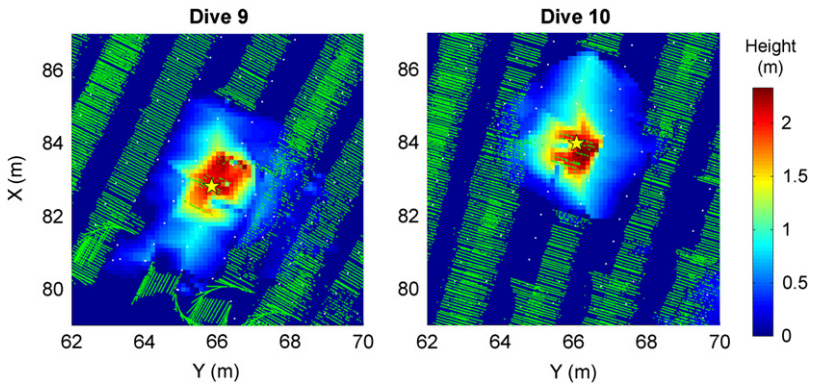

Fig. 11. Comparison of colony 12 between the two dives. Original bathymetry measurements by light-sectioning are shown by the green dots. The white dots represent bathymetry measurements by a DVL. The volumetric center of the colony is indicated by the yellow star. (For interpretation of the references to color in this figure legend, the reader is referred to the web version of this article.)

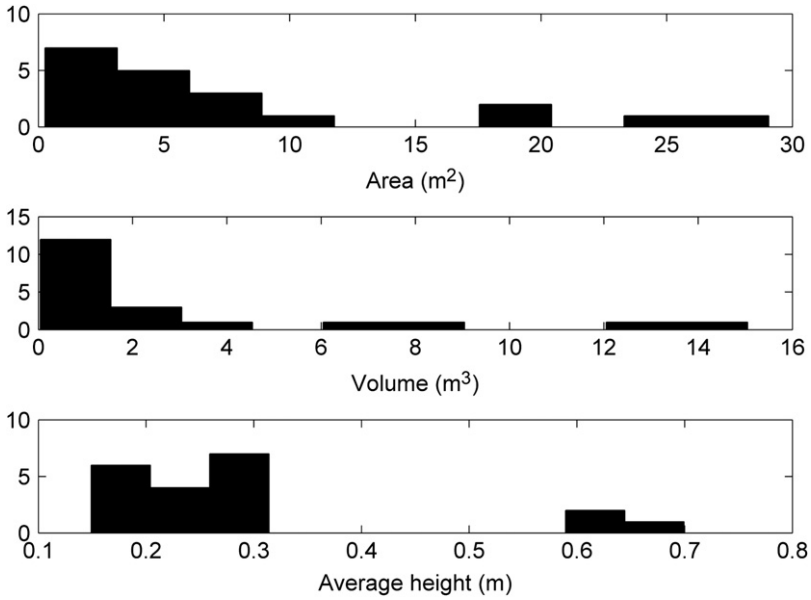

Fig. 12. Histograms of the morphological parameters of the numbered tubeworm colonies (except colony 18) shown in Fig. 9.

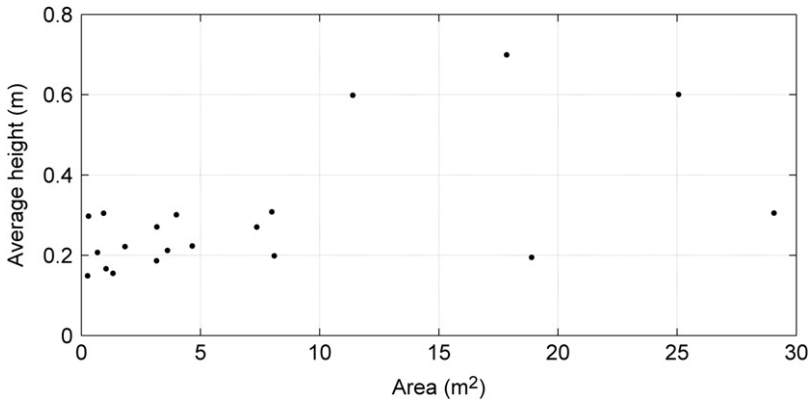

Fig. 13. Relationship between area and average height of the numbered tubeworm colonies (except colony 18) shown in Fig. 9.

separated into two groups. The shorter ones varied between 0.1 and 0.3 m, while the taller ones 0.6 and 0.7 m. Colonies numbered 10, 12, and 14 are belonged to the taller group. Although these colonies are located within a 15 m radius, the determinant factor of the average height seems to be complicated given that colonies 8 and 11 lay between the tall ones and had an average height of only 0.2 m. Fig. 13 shows the relationship between the area and average height. Although there is no strong positive correlation between them, all of the tall colonies had areas greater than 10 m^2.

4. Conclusions

This paper proposes a comprehensive method to measure the three-dimensional distribution of tubeworm colonies. The method consists of a real-time component for AUV navigation and a post-processing component for tubeworm detection. Quantitative measurements such as the volume and area of tubeworm colonies are obtained through dense low-altitude surveys by an AUV. The obtained data are processed using both geometric and visual features of tubeworm colonies. The proposed method was verified through observation of tubeworms at the Tagiri vent field in Kagoshima Bay, Japan, using the AUV *Tri-Dog* 1. The results revealed the spatial distribution of the shallow water tubeworm *L. satsuma* over an area as large as 2600 m^2. The overall footprint of the tubeworms was estimated to be 151.9 m^2, which is 5.8% of the observed area. The total number of tubes was estimated to be 99,500. The average height of the colonies could be separated into two groups of short (0.1–0.3 m) and tall (0.6–0.7 m), independent of the area. This type of information has rarely been available before. Therefore, the authors believe that the proposed method will bring about significant advances in marine benthic ecology.

Acknowledgments

The authors thank Drs. J. Hashimoto, K. Kubokawa, Y. Fujiwara, and T. Yamanaka, as well as the staff of the JAMSTEC R/V Tansei-Maru for their help and support (Cruise no. KT07-20). The bathymetry shown in Fig. 2 was obtained at the JAMSTEC research cruise NT05-12, 13. The authors also thank Dr. H. Singh and his colleagues for their helpful advices on creating photomosaics.

References

Boetius, A., 2005. Microfauna–macrofauna interaction in the seafloor: lessons from the tubeworm. Plos Biology 3 (3), 375–378.
Cardigos, F., Colaco, A., Dando, P., Avila, S., Sarradin, P., Tempera, F., Conceicao, P., Pascoal, A., Serraosantos, R., 2005. Shallow water hydrothermal vent field

fluids and communities of the D. João de Castro Seamount (Azores). Chemical Geology 224 (1–3), 153–168.
Courtney, L.A., Fisher, W.S., Raimondo, S., Oliver, L.M., Davis, W.P., 2007. Estimating 3-dimensional colony surface area of field corals. Journal of Experimental Marine Biology and Ecology 351 (1–2), 234–242.
Degraer, S., Moerkerke, G., Rabaut, M., Van Hoey, G., Du Four, I., Vincx, M., Henriet, J.P., Van Lancker, V., 2008. Very-high resolution side-scan sonar mapping of biogenic reefs of the tube-worm *Lanice conchilega*. Remote Sensing of Environment 112 (8), 3323–3328.
Falkowski, P., 2000. The global carbon cycle: a test of our knowledge of Earth as a system. Science 290 (5490), 291–296.
Fujikura, K., Okutani, T., Maruyama, T. (Eds.), 2008. Tokai University Press.
Hashimoto, J., Fujikura, K., Fujiwara, Y., Tanishima, M., Miura, T., Tsukahara, J., Ueno, H., Ossaka, J., Kikawada, K., 1995. Mapping of euchlanis communities in Kagoshima Bay (in Japanese). In: Proceedings of JAMSTEC Symposium On Deep Sea Research.
Hashimoto, J., Miura, T., Fujikura, K., Ossaka, J., 1993. Discovery of vestimentiferan tube-worms in the euphotic zone. Zoological Science 10 (6), 1063–1067.
Ierodiaconou, D., Burq, S., Reston, M., Laurenson, L., 2007. Marine benthic habitat mapping using multibeam data, georeferenced video and image classification techniques in Victoria, Australia. Journal of Spatial Science 52 (1), 93–104.
Ingole, B.S., Ansari, Z.A., Rathod, V., Rodrigues, N., 2001. Response of deep-sea macrobenthos to a small-scale environmental disturbance. Deep-Sea Research Part II—Topical Studies in Oceanography 48 (16), 3401–3410.
Johnson-Roberson, M., Pizarro, O., Williams, S.B., Mahon, I., 2010. Generation and visualization of large-scale three-dimensional reconstructions from underwater robotic surveys. Journal of Field Robotics 27 (1), 21–51.
Kondo, H., Maki, T., Ura, T., Nose, Y., Sakamaki, T., Inaishi, M., 2004. Relative navigation of an autonomous underwater vehicle using a light-section profiling system. Intelligent Robots and Systems, 2004. (IROS 2004). Proceedings. 2004 IEEE/RSJ International Conference on, pp. 1103-1108 vol. 1102.
Kondo, H., Ura, T., Nose, Y., 2001. Development of an autonomous underwater vehicle "Tri-Dog" toward practical use in shallow water. Journal of Robotics and Mechatronics 13 (2), 205–211.
Kostylev, V.E., Todd, B.J., Fader, G.B.J., Courtney, R.C., Cameron, G.D.M., Pickrill, R.A., 2001. Benthic habitat mapping on the Scotian Shelf based on multibeam bathymetry, surficial geology and sea floor photographs. Marine Ecology-Progress Series 219, 121–137.
Lebrato, M., Iglesias-Rodriguez, D., Feely, R.A., Greeley, D., Jones, D.O.B., Suarez-Bosche, N., Lampitt, R.S., Cartes, J.E., Green, D.R.H., Alker, B., 2010. Global contribution of echinoderms to the marine carbon cycle: $CaCO_3$ budget and benthic compartments. Ecological Monographs 80 (3), 441–467.
Maki, T., Kondo, H., Ura, T., Sakamaki, T., 2007a. Positioning method for an AUV using a profiling sonar and passive acoustic landmarks for close-range observation of seafloors. OCEANS 2007, Europe, pp. 1–6.
Maki, T., Kondo, H., Ura, T., Sakamaki, T., 2008. Large-area visual mapping of an underwater vent field using the AUV Tri-Dog. OCEANS 2008, pp. 1–8.
Maki, T., Mizushima, H., Kondo, H., Ura, T., Sakamaki, T., Yanagisawa, M., 2007b. Real time path-planning of an AUV based on characteristics of passive acoustic landmarks for visual mapping of shallow vent fields. OCEANS 2007, pp. 1–8.
Maki, T., Ura, T., Mizushima, H., Kondo, H., Sakamaki, T., Yanagisawa, M., 2007c. Low altitude tracking of rugged seafloors for autonomous visual observation. In: Underwater Technology and Workshop on Scientific Use of Submarine Cables and Related Technologies, 2007. Symposium on, pp. 488–494.
Miura, T., Tsukahara, J., Hashimoto, J., 1997. *Lamellibrachia satsuma*, a new species of vestimentiferan worms (Annelida: Pogonophora) from a shallow hydrothermal vent in Kagoshima Bay, Japan. Proceedings of the Biological Society of Washington 110 (3), 447–456.
Myers, M.R., Ambrose, R.F., 2009. Differences in benthic cover inside and outside marine protected areas on the Great Barrier Reef: influence of protection or disturbance history? Aquatic Conservation—Marine and Freshwater Ecosystems 19 (7), 736–747.
Nicholson, J.W., Healey, A.J., 2008. The present state of autonomous underwater vehicle (AUV) applications and technologies. Marine Technology Society Journal 42 (1), 44–51.
Pikitch, E.K., Santora, C., Babcock, E.A., Bakun, A., Bonfil, R., Conover, D.O., Dayton, P., Doukakis, P., Fluharty, D., Heneman, B., Houde, E.D., Link, J., Livingston, P.A., Mangel, M., McAllister, M.K., Pope, J., Sainsbury, K.J., 2004. Ecosystem-based fishery management. Science 305 (5682), 346–347.
Sanchez, F., Serrano, A., Ballesteros, M.G., 2009. Photogrammetric quantitative study of habitat and benthic communities of deep Cantabrian Sea hard grounds. Continental Shelf Research 29 (8), 1174–1188.
Singh, H., Armstrong, R., Gilbes, F., Eustice, R., Roman, C., Pizarro, O., Torres, J., 2004. Imaging coral I: imaging coral habitats with the SeaBED AUV. Subsurface Sensing Technologies and Applications 5 (1), 25–42.
Tarasov, V., Gebruk, A., Mironov, A., Moskalev, L., 2005. Deep-sea and shallow-water hydrothermal vent communities: two different phenomena? Chemical Geology 224 (1–3), 5–39.
Tetlow, S., Allwood, R.L., 1995. Development and applications of a novel underwater laser illumination system. Underwater Technology 21 (2), 13–20.
Yoerger, D.R., Jakuba, M., Bradley, A.M., Bingham, B., 2007. Techniques for deep sea near bottom survey using an autonomous underwater vehicle. International Journal of Robotics Research 26 (1), 41–54.